ELSEVIER

Journal of Nuclear Materials 275 (1999) 277–286

journal of nuclear materials

www.elsevier.nl/locate/jnucmat

Volatilization of urania in steam at elevated temperatures

Kenichi Hashizume[a,*], Wei-E Wang[b], Donald R. Olander[b]

[a] *Department of Advanced Energy Engineering Science, Kyushu University, Fukuoka 812-8581, Japan*
[b] *Department of Nuclear Engineering, University of California, Berkeley, CA 94720, USA*

Received 12 October 1998; accepted 6 May 1999

Abstract

The volatilization rates of urania in pure steam and in mixtures of steam and argon, steam and helium, and in steam/Ar/H_2 were measured in a thermogravimetric apparatus at atmospheric pressure and temperatures from 1250°C to 1600°C. The objective was to clarify the kinetics and mechanism of the volatilization process and to assess the validity of existing thermodynamic data that is needed to interpret the kinetic data. The mass transfer characteristics of the system were determined independently by measuring the evaporation rates of metals of well-known vapor pressures. The measurements of urania volatilization show that the rate-controlling process is gas-phase mass transfer of uranium-bearing species such as UO_3. Analysis of the volatilization data also suggests that the calculated UO_3 vapor pressures are somewhat in error at the lower temperatures in the range tested.

1. Introduction

Knowledge of the volatilization behavior of urania in steam is important in order to understand fuel behavior during severe accidents in water-cooled reactors. Due to the reaction of UO_2 with steam, fuel exposed at high temperatures would not only melt and relocate but partly volatilize as uranium compounds such as UO_3 and $UO_2(OH)_2$. Such volatile species would disperse in the gas and condense as aerosol particles which could transport fission products to low temperature zones.

Additionally, the volatilization of UO_2 plays a significant role in the direct release rate of fission products from the fuel. Analyses of radionuclide behavior under severe accident conditions have been conducted [1–3] on a basis of mass transfer theory, which relies on the thermodynamic data on uranium, in particular the equilibrium vapor pressures of UO_3 and $UO_2(OH)_2$. Although thermodynamic data on these species have been reported by many investigators [4–8], they are scattered and in some cases differ by two orders of magnitude at 1500 K. Recently, the existing thermodynamic data related to uranium volatilization in steam were reviewed by Olander [9] and the recommended data for calculating the partial pressure of the uranium-bearing vapors were proposed.

In the evaluation of volatilization of urania in steam, understanding of the mechanism is important. It is necessary to identify the rate-controlling process of the reaction. Experimental studies on volatilization of urania in air at high temperatures [10,11] have suggested that a surface chemical reaction is the rate-controlling process. Studies by other investigators [12,13] could not determine whether the rate-controlling process in steam is a surface chemical reaction or gas-phase mass transfer of the volatile species.

In order to clarify the rate-controlling process and to examine the validity of the thermodynamic data, the volatilization rates of urania in pure steam and in mixtures of steam/Ar, steam/He and steam/Ar/H_2 were measured in a thermogravimetric apparatus. In the analysis of the urania volatilization measurements, the thermodynamic data recommended by Olander [9] were adopted. Prior to performing the experiments, the gas-phase mass-transfer properties of the system were independently determined by a correlation giving the Sherwood number as a function of Schmidt and Reynolds numbers. The correlation was established by vaporizing pure metals whose vapor pressures are well known. Using this correlation to predict the rate of the mass transfer

* Corresponding author. Tel./fax: +81-92 642 3796.
E-mail address: hashi@nucl.kyushu-u.ac.jp (K. Hashizume)

0022-3115/99/$ - see front matter
PII: S0022-3115(99)00123-3

step, the mechanism of urania volatilization and the validity of thermodynamic data were elucidated.

2. Theoretical background

2.1. Equilibrium vapor pressure of uranium-bearing compounds

Since the principal vapor species UO_3 is considered to be produced by oxidizing UO_{2+x}, its partial pressure depends on the O_2 pressure. In steam, the O_2 pressure is governed by the decomposition reaction of steam. Therefore, the volatilization of urania in steam is governed by the following reactions, including the contribution of the oxyhydroxide:

$$H_2O\ (g) = H_2(g) + \frac{1}{2}O_2\ (g), \tag{1}$$

$$UO_2\ (s) + xH_2O\ (g) = UO_{2+x}\ (s) + xH_2\ (g), \tag{2}$$

$$UO_{2+x}\ (s) + (1-x)H_2O\ (g) = UO_3\ (g) + (1-x)H_2\ (g), \tag{3}$$

$$UO_3\ (g) + H_2O\ (g) = UO_2(OH)_2\ (g). \tag{4}$$

On a basis of the data recommended in Ref. [9], the relations among the oxygen partial pressure, P_{O_2}, the O/U ratio and the equilibrium vapor pressure of uranium-bearing compounds were evaluated. The equilibrium vapor pressures of UO_3 and $UO_2(OH)_2$ were summed to give the total equilibrium pressure of uranium-bearing vapors, $p(U)$.

2.2. Volatilization mechanism

If a surface chemical reaction between urania and steam is the rate-controlling process in volatilization, its rate m_i per unit surface area is expressed phenomenologically as a rate constant k_i times the difference between equilibrium vapor pressure of total gaseous uranium, $p(U)_{eq}$, and its actual partial pressure in the gas at the surface, $p(U)_i$:

$$m_i = k_i(p(U)_{eq} - p(U)_i)/RT, \tag{5}$$

where R is the gas constant and T is the absolute temperature. On the other hand, if mass transfer in the gas phase governs the volatilization, the flux m_m is expressed by

$$m_m = k_m(p(U)_i - p(U)_b)/RT, \tag{6}$$

where k_m is the mass-transfer coefficient. The vapor pressure of uranium compounds in the bulk gas, $p(U)_b$, can be neglected because the vapor of uranium compounds is diluted by a large amount of ambient gas in the present experiment. Since these two stages are in series (i.e. $m_i = m_m$), the relation between the experimentally obtained volatilization rate m_{exp} per unit surface area and the overall mass transfer coefficient K is expressed by

$$m_{exp} = K\,p(U)_{eq}/RT, \tag{7}$$

where

$$K = 1/(1/k_i + 1/k_m). \tag{8}$$

If the rate-controlling process is purely a surface reaction, the volatilization rate would be independent of gas flow rates and types of carrier gases. On the other hand, if the system is purely governed by the gas-phase mass transfer, the volatilization rate would depend on these variables. The mass-transfer characteristics can be expressed on a basis of a dimensionless correlation by the following equation [14]:

$$Sh = A\,Re^a\,Sc^b, \tag{9}$$

where Sh is the Sherwood number (k_mL/D), Re is the Reynolds number (VL/v), Sc is the Schmidt number (v/D), L is the characteristic dimension of the specimen, V is the gas flow velocity, D is the diffusion coefficient of the volatile substance in the gas phase, v is the kinematic viscosity of gas, and A, a and b are the constants.

The flow geometry and specimen shape in the present experiment resemble laminar flow parallel to a flat plate. In this case, the constants, A, a and b are theoretically equal to 0.664, 1/2 and 1/3, respectively [14]. However, since the constants depend on the details of the geometry of the specimen and the apparatus, the constants in Eq. (9) have to be determined independently by tests using substances whose volatilization is free from surface reaction restrictions. The pure metals Fe and Cr were selected for this purpose because they have adequately high vapor pressures in the temperature region investigated. The mass transfer coefficient in the metal evaporation tests is obtained from the analog of Eq. (6):

$$k_m = RTm_{metal}/P_{metal}, \tag{10}$$

where m_{metal} is the metal evaporation flux and P_{metal} is its vapor pressure at temperature T. P_{metal} is equal to the partial pressure of the metal at the surface of the solid. The partial pressure of the metal vapor in the bulk gas is zero as mentioned above.

The results of the metal vaporization tests are utilized to determine the constants in Eq. (9). The resulting correlation is then used to calculate the expected gas-phase mass-transfer coefficient for UO_2 volatilization, k_m^{th}. The overall rate coefficients K determined from the experimental rates m_{exp} and the literature estimates of the equilibrium total pressures of uranium-bearing vapor $p(U)_{eq}$ are compared to the expected values of k_m^{th}.

If K is significantly less than k_m^{th}, the existence of a slow surface chemical step is inferred. If $K \approx k_m^{th}$, the process is mass-transfer limited and the estimated equilibrium pressures $p(U)_{eq}$ and the gas transport properties D and ν are accurate. If the measured K values exceed k_m^{th}, the most likely explanation is that the volatilization is gas-phase mass-transfer limited but the UO_3 and $UO_2(OH)_2$ equilibrium pressures taken from the literature are too low k_m^{th}.

3. Experimental

Fig. 1 shows the schematic diagram of the thermogravimetric apparatus (TGA) for both the metal evaporation and the urania volatilization experiments. It is equipped with a microbalance and a gas-flow system. The gas-flow lines are heated to more than 200°C to prevent steam from condensing. A dense alumina tube, the inner diameter of which is 9.6 mm, is used as the furnace tube. The temperature of the furnace is controlled by thermocouples inserted in the furnace but outside the furnace tube. Prior to the experiments, these thermocouples were calibrated by thermocouples inserted inside the furnace tube at the position of the specimen. The calibration was performed varying the types and flow rates of the gases.

3.1. Vaporization of iron and chromium

Slab-shaped specimens of Fe and Cr were prepared in order to examine the mass-transfer characteristics of the TGA. The specimen size was $1\times3\times10$ mm^3 with a 1 mm hole bored at one end to hook to a tungsten hangdown wire from the microbalance. In order to prevent the specimens from oxidizing, He or Ar with 4% H_2 were used as the ambient gas. In addition, zirconium lumps were added in the alumina preheating bed of the furnace tube as an oxygen getter. The metal vaporization experiments were carried out at 1500°C at a flow rate from 50 to 200 ccm (at room temperature) which corresponded to an average velocity from 7 to 28 cm/s. The signals of the weight change of the specimen from the microbalance were recorded on a personal computer.

3.2. Volatilization of urania

UO_2 specimens ($1\times3\times10$ mm^3, 97% theoretical density) were suspended in the apparatus by a Pt or Pt–Ir alloy chain. In order to prevent reaction between the specimen and the Pt chain, a connecting alumina ring was used. The volatilization experiments were carried out at gas flow rates from 50 to 200 ccm in a temperature region from 1250°C to 1600°C. Pure steam or a mixture of steam/He, steam/Ar or steam/Ar/H_2 was chosen as the ambient gas. Ar with 4% H_2 added was used as a sweep gas before and after the steam-containing gas

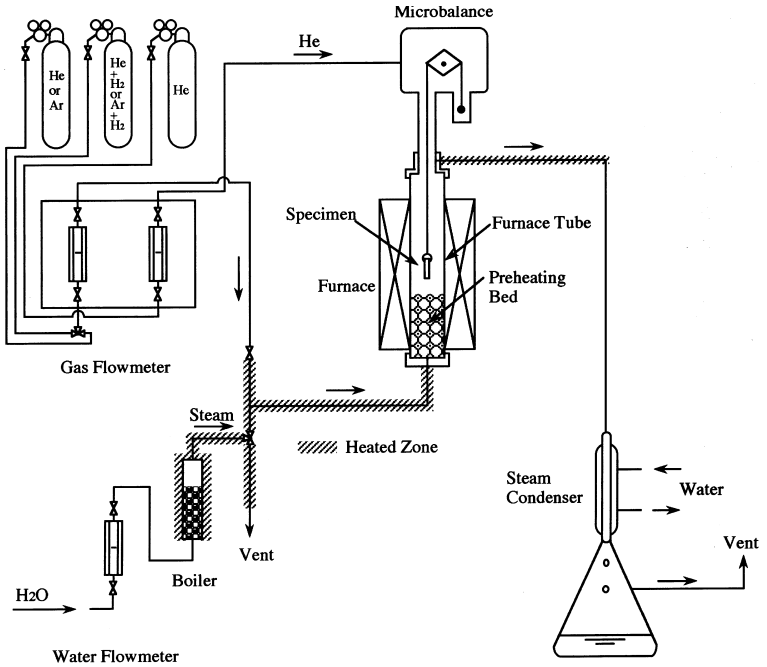

Fig. 1. Schematic diagram of the thermogravimetric apparatus.

flow. Volatilization in steam was observed as a constant weight loss rate following an initial transient in which UO_2 oxidized to the equilibrium UO_{2+x}. At the end of an experiment, the UO_{2+x} produced in steam was reduced to UO_2 in the Ar/H_2 gas mixture.

4. Results and discussion

4.1. Determination of the mass-transfer correlation from the metal evaporation tests

Using Eq. (10), the experimental mass-transfer coefficient k_m^{exp} was calculated from the vaporization rate m_{exp} and the vapor pressure of the metal at 1500°C (1.40×10^{-5} atm and 7.76×10^{-5} atm for Fe and Cr, respectively). The theoretically expected mass-transfer coefficient k_m^{th} was also calculated from Eq. (9). The data for the vaporization of Fe and Cr are listed in Appendix A, which includes the diffusivity D of the metals and the viscosity v of the gases calculated on a basis of the theoretical treatment and thermodynamic data of Refs. [15–17]. In the calculation, the influence of the hydrogen added in the inert gases on the diffusivity and the viscosity was neglected because its content was low. The experimental data are compared to theory in Fig. 2, in which the solid line is based on Eq. (9) for a flat plate and the dotted lines represent the standard deviation of the data. As seen in this figure, the experimental data are scattered around the theoretical line. The chief cause of the scattering is the off-center position and/or vibration of the specimen in the furnace tube during the experiment. These are due to the relatively high flow rates needed in order to avoid natural convection of the gas in the tube.

The experimental Sherwood numbers follow the theoretical dependence on the Schmidt and Reynolds numbers. The fact that the constant A is virtually identical to that for laminar flow over a flat plate is fortuitous because the specimen is a rectangular parallelpiped. Nevertheless, the constants, $A=0.664$, $a=1/2$ and $b=1/3$, in conjunction with Eq. (9), are adopted in the following analysis of urania volatilization.

4.2. Volatilization of urania

An example of the weight change of specimen is shown in Fig. 3. Switching the gas from Ar/H_2 to steam leads to a weight gain due to oxidation reaction based on Eq. (2) and then a weight loss based on Eqs. (3) and (4). Returning to Ar/H_2 at 11 000 s results in a weight loss based on the reverse reaction of Eq. (2). The characteristics of such a volatilization of urania in steam are exhibited in Figs. 4 and 5, in which the lines are drawn for a visual guide. As seen in these figures, volatilization rates depend significantly on the flow rates and the types of gases: the rate increases with the gas flow rate, and is greater in He stream than in Ar stream. These experimental results suggest that the rate-controlling process is gas-phase mass transfer rather than a surface chemical reaction between urania and steam.

Cox et al. [11] have reported porous structure of urania surface after volatilization experiments at temperatures above 1800°C in air, which suggested that the rate-limiting process is a surface reaction. Fig. 6 shows micrographs of the surfaces of the urania specimens from this study after volatilization experiments in steam at 1300°C and 1600°C. In both cases, appreciable grain

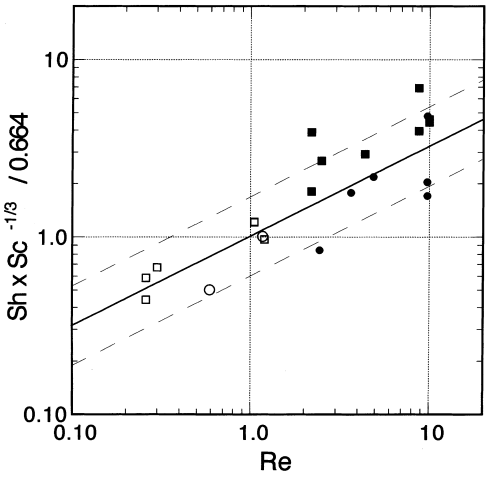

Fig. 2. Mass-transfer coefficients for the vaporization of Fe and Cr at 1500°C. Open circles: Fe in He; closed circles: Fe in Ar; open squares: Cr in He; closed squares: Cr in Ar.

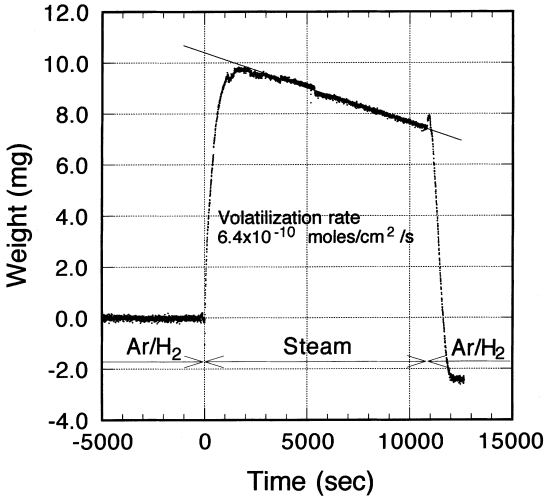

Fig. 3. Weight change of urania in pure steam at 1400°C.

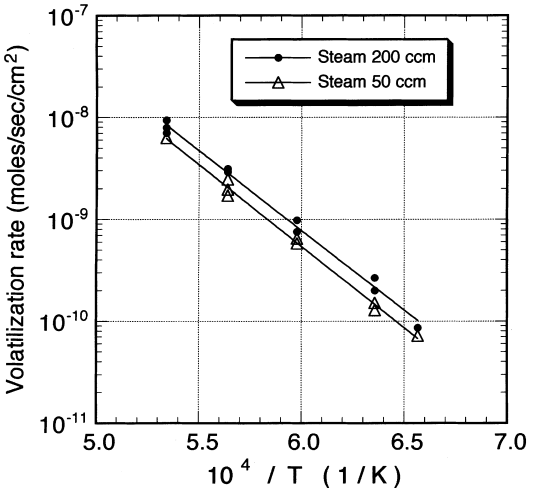

Fig. 4. Volatilization rate of urania in pure steam at flow rates of 50 and 200 ccm.

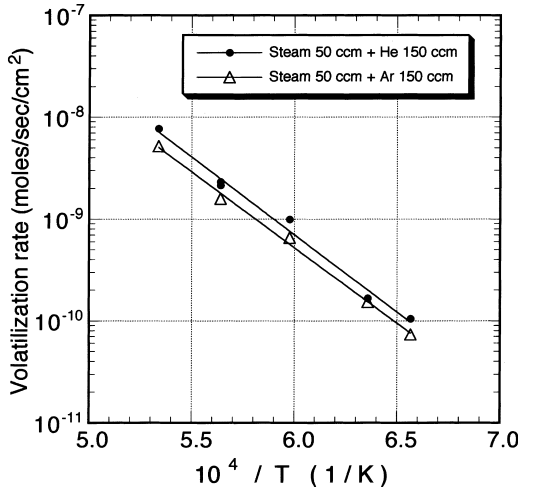

Fig. 5. Volatilization rate of urania in steam/He and steam/Ar at 200 ccm.

growth occurred. However, the porous structure reported by Cox et al. was not observed.

Fig. 7 illustrates the effect of hydrogen on the volatilization rate. As expected from the thermodynamic data [9], addition of hydrogen to steam significantly decreases $p(U)_{eq}$ and hence reduces the volatilization rate. This suggests that during a severe accident the hydrogen gas generated by the reaction of steam with Zircaloy cladding would drastically suppress the volatilization of urania.

Because of the clear dependence of the volatilization rate on the gas flow rate and the type of inert gas, the interpretation of the data was based strictly on mass-transfer theory. Experimental mass-transfer coefficients were calculated from Eq. (7) with $K = k_m^{exp}$. The equilibrium pressure $p(U)_{eq}$ was determined for each gas composition and temperature using the thermodynamic data recommended by Olander [9]. Since the equilibrium vapor pressure of $UO_2(OH)_2$ is relatively low in the present experimental condition, the main uranium-bearing compound is UO_3. The equilibrium vapor pressure of UO_3, P_{UO_3}, and $p(U)_{eq}$ are listed in Appendix B. The resulting experimental mass-transfer coefficients were then converted to the ordinate used in Fig. 2 for metal evaporation, namely $Sh\ Sc^{-1/3}/0.664$.

In the analysis, the diffusion coefficient D and the viscosity v were calculated on a basis of the theoretical treatment in Ref. [15] because there are no adequate experimental data for them, in particular, D. The diffusivity of the uranium-bearing compound was evaluated in the same manner as Fe and Cr. For UO_3 and $UO_2(OH)_2$, however, the thermodynamic data needed to

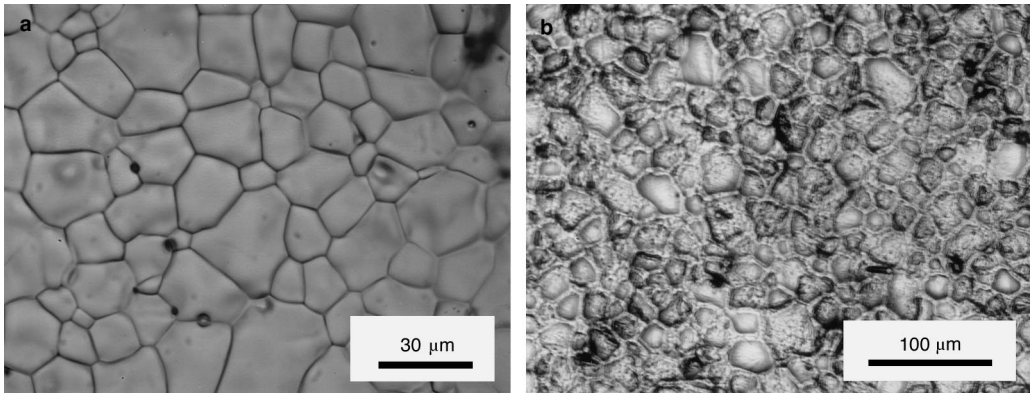

Fig. 6. Optical micrographs of specimen surface after reaction with steam at (a) 1300°C and (b) 1600°C.

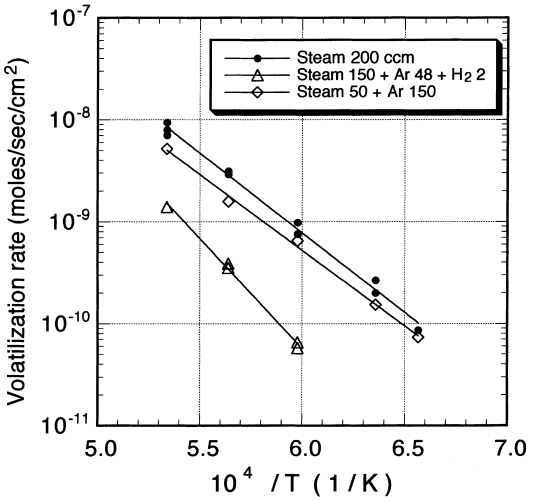

Fig. 7. Effect of hydrogen on volatilization rate of urania.

estimate D are not available, although such data are available for UO_2. Therefore the thermodynamic data of UO_2 were substituted for that of the volatile uranium compounds. Additionally, the main uranium-bearing compound in the present experimental condition is UO_3. Therefore, the diffusivity of UO_3 calculated from the thermodynamic data of UO_2 was adopted.This substitution should be reasonable because the diffusivity mainly depends on the molecular weight of gas component rather than its thermodynamic parameters: the molecular weight of UO_3 is not very different from those of UO_2 and $UO_2(OH)_2$. In the case of gas mixtures, such as steam/He and steam/Ar, the viscosity v and the diffusivity D were evaluated on a basis of the theoretical treatment of gas mixtures [15]. The data for the mass-transfer analysis of the volatilization of urania in stream are given in Appendix B. The result of the dimensional analysis is exhibited in Fig. 8, where the data for Fe and Cr and the standard deviation are included for comparison. As seen in this figure, points for the volatilization of urania are almost parallel to the theoretical (i.e. metal-based) line, which means that the volatilization rate is governed by the mass transfer of gaseous products. The discrepancy between the experimental data and the metal-based line is significant but not excessive. This suggests that the thermodynamic data adopted (including the effect of hydrogen) and the mass-transfer properties are reasonably valid. However, the experimental data for urania are more scattered than the metal data, and are shifted upward from the latter. The lower-temperature data deviate more from the theoretical line than the data at the highest temperature investigated. Fig. 9 shows the ratio of the experimental mass-transfer coefficient k_m^{exp} to theoretically expected value k_m^{th} as a function of temperature. From this figure, it is clear that the deviation at lower temperatures is the principal cause of the deviation of the UO_2 data from the metal data in Fig. 8. This implies that thermodynamic data, such as vapor pressure of UO_3 and the contribution of $UO_2(OH)_2$, and/or the transport properties, the diffusivity D and the viscosity v of the gas, are somewhat in error at lower temperatures. Underestimation of the vapor pressure of UO_3 or of the contribution of $UO_2(OH)_2$ would cause the upward shift of the points from the theoretical line in Fig. 8. The temperature dependence of the diffusivity D and the viscosity v is not large enough to cause the strong temperature effect seen in Fig. 9: D and v are roughly proportional to $T^{3/2}$ and $T^{1/2}$, respectively [15]. The ordinate of Fig. 8 varies as $D^{-2/3}$, which means a temperature dependence of $1/T$.

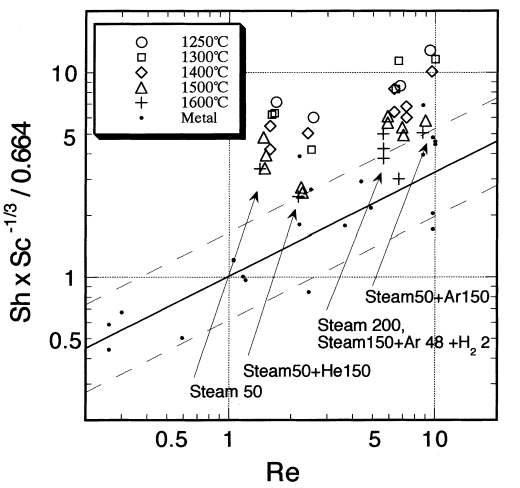

Fig. 8. Mass-transfer coefficients for volatilization of urania in steam, steam/He, steam/Ar and steam/Ar/H_2.

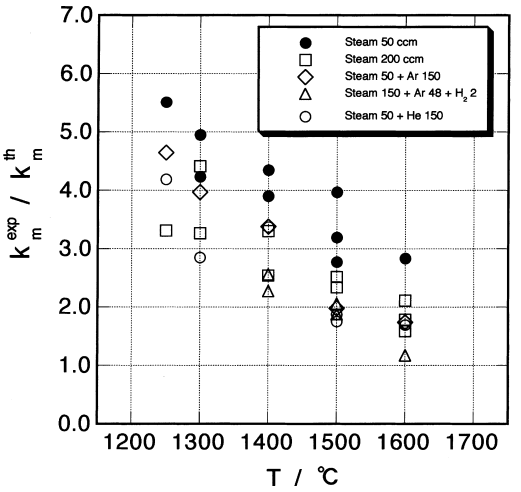

Fig. 9. Deviation of mass-transfer coefficient from the theoretical value based on metal evaporation tests.

Table 1
Data on vaporization of Fe and Cr

Run no.	Gas (ccm)	V (cm/s)	m_{metal} (mol/s/cm^2)	v (cm^2/s)	D (cm^2/s)	P_{metal} (atm)	k_m^{exp} (cm/s)	k_m^{th} (cm/s)	k_m^{exp}/k_m^{th}	Re	Sh	Sc
FE08-1	Ar 200	27.8	8.98×10^{-10}	2.80	2.90	1.40×10^{-5}	9.33	6.07	1.54	9.74	3.15	0.964
FE10-1	Ar 200	27.8	3.21×10^{-10}	2.80	2.90	1.40×10^{-5}	3.33	6.07	0.55	9.74	1.12	0.964
FE10-3	Ar 200	27.8	3.83×10^{-10}	2.80	2.90	1.40×10^{-5}	3.98	6.07	0.66	9.74	1.34	0.964
FE08-3-1	Ar 100	13.9	4.09×10^{-10}	2.80	2.90	1.40×10^{-5}	4.25	4.29	0.99	4.87	1.43	0.964
FE08-3-2	Ar 75	10.4	3.33×10^{-10}	2.80	2.90	1.40×10^{-5}	3.46	3.71	0.93	3.65	1.17	0.964
FE10-2	Ar 50	7.0	1.58×10^{-10}	2.80	2.90	1.40×10^{-5}	1.64	3.04	0.54	2.44	0.555	0.964
FE08-2-1	He 200	27.8	1.02×10^{-9}	23.3	12.7	1.40×10^{-5}	10.6	11.4	0.93	1.17	0.820	1.83
FE08-2-2	He 100	13.9	5.10×10^{-10}	23.3	12.7	1.40×10^{-5}	5.30	8.09	0.66	0.590	0.410	1.83
CR06-2	Ar 200	27.8	4.77×10^{-9}	2.80	3.09	7.76×10^{-5}	8.93	6.67	1.34	8.74	2.54	0.905
CR08-3	Ar 200	27.8	8.33×10^{-9}	2.80	3.09	7.76×10^{-5}	15.6	6.67	2.34	8.74	4.44	0.905
CR09-2	Ar 200	27.8	4.68×10^{-9}	2.80	3.09	7.76×10^{-5}	8.78	6.24	1.40	9.99	2.85	0.905
CR09-5	Ar 200	27.8	4.83×10^{-9}	2.80	3.09	7.76×10^{-5}	9.06	6.24	1.45	9.99	2.95	0.905
CR06-3	Ar 100	13.9	3.53×10^{-9}	2.80	3.09	7.76×10^{-5}	6.61	4.71	1.40	4.37	1.88	0.905
CR06-1	Ar 50	7.0	2.17×10^{-9}	2.80	3.09	7.76×10^{-5}	4.06	3.34	1.22	2.19	1.16	0.905
CR08-4	Ar 50	7.0	4.69×10^{-9}	2.80	3.09	7.76×10^{-5}	8.78	3.34	2.63	2.19	2.50	0.905
CR09-1	Ar 50	7.0	2.82×10^{-9}	2.80	3.09	7.76×10^{-5}	5.28	3.12	1.69	2.50	1.72	0.905
CR07-2	He 200	27.8	7.89×10^{-9}	23.3	13.3	7.76×10^{-5}	14.7	12.4	1.19	1.05	0.976	1.75
CR08-2	He 200	27.8	7.80×10^{-9}	23.3	13.3	7.76×10^{-5}	14.6	12.4	1.18	1.05	0.967	1.75
CR09-3	He 200	27.8	5.47×10^{-9}	23.3	13.3	7.76×10^{-5}	10.3	11.6	0.89	1.20	0.776	1.75
CR07-1	He 50	7.0	2.86×10^{-9}	23.3	13.3	7.76×10^{-5}	5.35	6.16	0.87	0.260	0.354	1.75
CR08-1	He 50	7.0	3.79×10^{-9}	23.3	13.3	7.76×10^{-5}	7.09	6.16	1.15	0.260	0.470	1.75
CR09-4	He 50	7.0	3.81×10^{-9}	23.3	13.3	7.76×10^{-5}	7.13	5.80	1.23	0.300	0.539	1.75

Table 2
Data on volatilization of urania in steam

Run no.	Temp. (K)	Gas (ccm)	V (cm/s)	m_{exp} (mol/s/cm^2)	ν (cm^2/s)	D (cm^2/s)	P_{O_2} (atm)	O/U	P_{UO_3} (atm)	$p(U)_{eq}$ (atm)	k_m^{exp} (cm/s)	k_m^{th} (cm/s)	k_m^{exp}/k_m^{th}	Re	Sh	Sc
UO14-1	1523	Steam 50	6.0	7.16×10^{-11}	3.69	1.31	1.28×10^{-4}	2.19	9.14×10^{-7}	1.06×10^{-6}	8.45	1.53	5.51	1.69	6.71	2.81
UO16-1	1523	Steam 200	23.9	8.60×10^{-11}	3.69	1.31	1.28×10^{-4}	2.19	9.14×10^{-7}	1.06×10^{-6}	10.1	3.07	3.31	6.76	8.07	2.81
UO14-2	1523	Steam 50 + He 150	23.9	1.04×10^{-10}	9.75	3.15	5.09×10^{-5}	2.165	6.39×10^{-7}	6.65×10^{-7}	19.6	4.68	4.19	2.56	6.49	3.09
UO15-2	1523	Steam 50 + Ar 150	23.9	7.32×10^{-11}	2.43	1.19	5.09×10^{-5}	2.165	6.39×10^{-7}	6.65×10^{-7}	13.7	2.96	4.65	9.44	12.0	2.03
UO03-1	1573	Steam 50	6.2	1.50×10^{-10}	3.89	1.40	1.95×10^{-4}	2.185	2.18×10^{-6}	2.41×10^{-6}	8.12	1.64	4.95	1.61	5.79	2.77
UO17-2	1573	Steam 50	6.2	1.28×10^{-10}	3.8	1.40	1.95×10^{-4}	2.185	2.18×10^{-6}	2.41×10^{-6}	6.84	1.61	4.23	1.66	5.09	2.77
UO02-1	1573	Steam 200	24.7	2.00×10^{-10}	3.89	1.40	1.95×10^{-4}	2.185	2.18×10^{-6}	2.41×10^{-6}	10.7	3.27	3.27	6.44	7.73	2.77
UO17-1	1573	Steam 200	24.7	2.66×10^{-10}	3.89	1.40	1.95×10^{-4}	2.185	2.18×10^{-6}	2.41×10^{-6}	14.2	3.23	4.41	6.65	10.6	2.77
UO17-3	1573	Steam 50 + He150	24.7	1.67×10^{-10}	10.3	3.35	7.73×10^{-5}	2.165	1.50×10^{-6}	1.54×10^{-6}	14.0	4.91	2.85	2.51	4.35	3.06
UO17-4	1573	Steam 50 + Ar150	24.7	1.53×10^{-10}	2.58	1.27	7.73×10^{-5}	2.165	1.50×10^{-6}	1.54×10^{-6}	12.8	3.22	3.97	10.0	10.5	2.03
UO04-1	1573	Steam 100+Ar 96 + H_2 4	24.7	No weight loss												
UO08-1	1673	Steam 50	6.6	6.47×10^{-10}	4.33	1.59	4.17×10^{-4}	2.175	1.09×10^{-5}	1.15×10^{-5}	7.72	1.77	4.35	1.58	5.06	2.72
UO18-1	1673	Steam 50	6.6	5.81×10^{-10}	4.33	1.59	4.17×10^{-4}	2.175	1.09×10^{-5}	1.15×10^{-5}	6.93	1.77	3.90	1.58	4.55	2.72
UO07-1	1673	Steam 200	26.3	9.84×10^{-10}	4.33	1.59	4.17×10^{-4}	2.175	1.09×10^{-5}	1.15×10^{-5}	11.7	3.55	3.30	6.33	7.70	2.72
UO18-4	1673	Steam 200	26.3	7.56×10^{-10}	4.33	1.59	4.17×10^{-4}	2.175	1.09×10^{-5}	1.15×10^{-5}	9.02	3.55	2.54	6.33	5.92	2.72
UO18-2	1673	Steam 50 + He150	26.3	9.88×10^{-10}	11.4	3.76	1.65×10^{-4}	2.155	7.37×10^{-6}	7.47×10^{-6}	18.1	5.38	3.37	2.41	5.03	3.02
UO18-3	1673	Steam 50 + Ar150	26.3	6.53×10^{-10}	2.84	1.42	1.65×10^{-4}	2.155	7.37×10^{-6}	7.47×10^{-6}	12.0	3.54	3.38	9.64	8.78	2.00
UO-BA-3	1673	Steam 150 + Ar 48 + H_2 2	26.3	6.53×10^{-11}	3.69	1.53	1.63×10^{-6}	2.06	9.31×10^{-7}	9.70×10^{-7}	9.24	3.61	2.56	7.24	6.14	2.41
UO21-1	1673	Steam 150 + Ar 48 + H_2 2	26.3	5.74×10^{-11}	3.69	1.53	1.63×10^{-6}	2.06	9.31×10^{-7}	9.70×10^{-7}	8.17	3.60	2.27	7.27	5.42	2.41
UO09-1	1773	Steam 50	7.0	2.46×10^{-9}	4.81	1.79	8.17×10^{-4}	2.165	4.43×10^{-5}	4.58×10^{-5}	7.82	1.97	3.97	1.47	4.44	2.69
UO19-1	1773	Steam 50	7.0	1.71×10^{-9}	4.81	1.79	8.17×10^{-4}	2.165	4.43×10^{-5}	4.58×10^{-5}	5.42	1.95	2.77	1.49	3.13	2.69
UO18-6	1773	Steam 50	7.0	1.95×10^{-9}	4.81	1.79	8.17×10^{-4}	2.165	4.43×10^{-5}	4.58×10^{-5}	6.21	1.94	3.19	1.51	3.62	2.69
UO-BA-1	1773	Steam 200	27.8	3.11×10^{-9}	4.81	1.79	8.17×10^{-4}	2.165	4.43×10^{-5}	4.57×10^{-5}	9.90	3.93	2.51	5.87	5.62	2.69

Table 2 (Continued)

Run no.	Temp. (K)	Gas (ccm)	V (cm/s)	m_{exp} (mol/s/cm^2)	v (cm^2/s)	D (cm^2/s)	P_{O_2} (atm)	O/U	P_{UO_3} (atm)	$p(U)_{eq}$ (atm)	k_m^{exp} (cm/s)	k_m^{th} (cm/s)	k_m^{exp}/k_m^{th}	Re	Sh	Sc
UO11-1	1773	Steam 200	27.8	2.91×10^{-9}	4.81	1.79	8.17×10^{-4}	2.165	4.43×10^{-5}	4.58×10^{-5}	9.21	3.94	2.34	5.87	5.23	2.69
UO12-1	1773	Steam 50 + He150	27.8	2.31×10^{-9}	12.6	4.20	3.24×10^{-4}	2.15	2.99×10^{-5}	3.02×10^{-5}	11.1	5.93	1.87	2.24	2.69	3.00
UO19-2	1773	Steam 50 + He150	27.8	2.14×10^{-9}	12.6	4.20	3.24×10^{-4}	2.15	2.99×10^{-5}	3.02×10^{-5}	10.3	5.88	1.75	2.27	2.53	3.00
UO19-3	1773	Steam 50 + Ar150	27.8	1.58×10^{-9}	3.14	1.59	3.24×10^{-4}	2.15	2.99×10^{-5}	3.02×10^{-5}	7.61	3.85	1.98	8.98	4.94	1.99
UO-BA-2	1773	Steam 150+ Ar 48 + H_2 2	27.8	3.90×10^{-10}	4.08	1.71	1.23×10^{-5}	2.09	6.84×10^{-6}	7.00×10^{-6}	8.10	3.94	2.06	6.91	4.80	2.38
UO19-4	1773	Steam 150 + Ar 48 + H_2 2	27.8	3.53×10^{-10}	4.08	1.71	1.23×10^{-5}	2.09	6.84×10^{-6}	7.00×10^{-6}	7.33	3.91	1.88	7.01	4.41	2.38
UO22-1	1873	Steam 50	7.3	6.26×10^{-9}	5.32	1.99	1.49×10^{-3}	2.16	1.56×10^{-4}	1.59×10^{-4}	6.06	2.14	2.84	1.41	3.10	2.67
UO13-1	1873	Steam 200	29.4	9.35×10^{-9}	5.32	1.99	1.49×10^{-3}	2.16	1.56×10^{-4}	1.59×10^{-4}	9.05	4.29	2.11	5.60	4.60	2.67
UO-BA-4	1873	Steam 200	29.4	7.91×10^{-9}	5.32	1.99	1.49×10^{-3}	2.16	1.56×10^{-4}	1.59×10^{-4}	7.66	4.29	1.79	5.61	3.90	2.67
UO22-4	1873	Steam 200	29.4	7.03×10^{-9}	5.32	1.99	1.49×10^{-3}	2.16	1.56×10^{-4}	1.59×10^{-4}	6.80	4.29	1.59	5.61	3.48	2.67
UO22-2	1873	Steam 50 + He150	29.4	7.68×10^{-9}	13.8	4.65	5.93×10^{-4}	2.135	1.08×10^{-4}	1.08×10^{-4}	10.9	6.41	1.70	2.17	2.39	2.97
UO22-3	1873	Steam 50 + Ar150	29.4	5.17×10^{-9}	3.44	1.75	5.93×10^{-4}	2.135	1.08×10^{-4}	1.08×10^{-4}	7.34	4.22	1.74	8.72	4.27	1.96
UO22-5	1873	Steam 150 + Ar 48 + H_2 2	29.4	1.39×10^{-9}	4.50	1.91	7.49×10^{-5}	2.095	4.22×10^{-5}	4.28×10^{-5}	5.01	4.27	1.17	6.66	2.68	2.36

This cannot account for the 2- and 3-fold variation over the temperature range from 1250°C to 1600°C seen in Fig. 9.

Although the volatilization rates in gases with H_2 added are an order of magnitude lower than the rates in steam (Fig. 7), points for the former in Fig. 8 fall well within the spread of points for the latter. This indicates that the thermodynamic effect of H_2 on the equilibrium UO_3 pressure is satisfactorily accounted for in the method recommended in Ref. [9].

In any case, it can be safely concluded that the rate-controlling process of urania volatilization in steam is mass transfer in the gas phase. The discrepancy of the volatilization rate between the experimental data and the theoretical (metal-based) value means that the use of the thermodynamic data recommended in Ref. [9] somewhat underestimates the amount of volatilized urania in severe accident analyses, especially in the lower temperature region.

5. Conclusions

1. The volatilization rates of urania in steam and in mixtures of steam/Ar, steam/He and steam/Ar/H_2 were measured by means of the micro-thermogravimetry at atmospheric pressure in a temperature region from 1250°C to 1600°C.
2. Comparison of urania volatilization with metal vaporization of identical flow geometry, specimen size and shape, temperature, and gas type and flow rate demonstrated that:
   - The rate-controlling process of the volatilization of urania in steam is mass transfer of uranium-bearing vapors in the gas phase.
   - The existing data for the equilibrium vapor pressure of UO_3, are too low, particularly at lower temperatures.
3. During a severe accident the hydrogen gas generated by the reaction of steam with Zircaloy cladding would drastically suppress the volatilization of urania.

Appendix A

Table 1 presents the data on vaporization of Fe and Cr.

Appendix B

The data on volatilization of urania in steam are presented in Table 2.

References

[1] T.J. Heames et al., VICTORIA: A mechanistic model of radionuclide behavior under severe accident conditions, Nuclear Regulatory Commission Report NUREG/CR-5545, 1992.
[2] V. Ozrin et al., Models for release of low-volatile fission products, Nuclear Safety Institute of the Russian Academy of Sciences NSI-SARR-43-96, 1996.
[3] B.J. Lewis, B.J. Corse, W.T. Thompson, M.H. Kaye, F.C. Iglesias, P. Elder, R. Dickson, Z. Liu, J. Nucl. Mater. 252 (1998) 235.
[4] P.E. Blackburn, J. Nucl. Mater. 46 (1973) 244.
[5] R.J. Ackermann, A.T. Chang, J. Chem. Thermo. 5 (1973) 873.
[6] T.B. Lindemer, T.M. Besmann, J. Nucl. Mater. 74 (1985) 472.
[7] O.H. Krikorian, B.B. Ebbinghaus, M.G. Adamson, A.S. Fortes, Jr., D.L. Fleming, Experimental studies and thermodynamic modeling of volatilities of uranium, plutonium, and americium from their oxides, Lawrence Livermore National Laboratory Report UCRL-ID-114774, 1993.
[8] B.B. Ebbinghaus, Calculated thermodynamic functions for gas-phase uranium, neptunium, plutonium, and americium oxides, oxyhydroxides, oxychlorides, and oxyfluorides, Lawrence Livermore National Laboratory Report UCRL-JC-122278, 1995.
[9] D.R. Olander, J. Nucl. Mater. 270 (1999) 187.
[10] C.A. Alexander, J.S. Ogden, High Temperature–High Pressures 22 (1990) 149.
[11] D.S. Cox, C.E.L. Hunt, Z. Liu, F.C. Iglesias, N.A. Keller, R.D. Barrand, R.F. O'Connor, A model for the release of low-volatility fission products in oxidizing conditions, Atomic Energy of Canada Ltd. Report AECL-10440, 1991.
[12] J. Abrefah, A. de Aguiar Braid, W. Wang, Y. Khalil, D.R. Olander, J. Nucl. Mater. 208 (1994) 98.
[13] B.J. Lewis, B. Andre, B. Morel, P. Dehaudt, D. Maro, P.L. Purdy, D.S. Cox, F.C. Iglesias, M.F. Osborne, R.A. Lorenz, J. Nucl. Mater. 227 (1995) 83.
[14] C.O. Bennett, J.E. Myers, Momentum, Heat and Mass Transfer, McGraw-Hill, New York, 1962.
[15] R.C. Reid, T.K. Sherwood, The Properties of Gases and Liquids, McGraw-Hill, New York, 1958.
[16] T. Iida, R.I.L. Guthrie, The Physical Properties of Liquid Metals, Clarendon, Oxford, 1988.
[17] R. Speiser, H.L. Johnson, P. Blackburn, J. Am. Chem. Soc. 72 (1950) 4142.